Synthesis and pH-dependent micellization of diblock copolymer mixtures.

Kathy van Butsele, Pierre Sibret, Charles-André Fustin, Gohy Jean-François, Catherine Passirani, Jean-Pierre Benoit, Jérôme Robert, Christine Jérôme

Synthesis and pH-dependent micellization of diblock copolymer mixtures

K. Van Butsele[a], P. Sibret[a], C. A. Fustin[b], J.F. Gohy[b], C. Passirani[c], J-P. Benoit[c], R. Jérôme[a], C. Jérôme[a]*

[a] Center for Education and Research on Macromolecules, Université de Liège, B6 Sart-Tilman, B-4000 Liege, Belgium, e-mail*: c.jerome@ulg.ac.be

[b] Unité CMAT, Université catholique de Louvain, Place Pasteur 1, 1348 Louvain-la-Neuve, Belgium

[c] INSERM U 646, 10 rue A. Boquel, 49000 Angers, France

* to whom correspondence should be sent

Abstract

This work focused on the preparation and the aqueous solution properties of hybrid polymeric micelles consisting of a hydrophobic poly(ε-caprolactone) (PCL) core and a mixed shell of hydrophilic poly(ethylene oxide) (PEO) and pH-sensitive poly(2-vinylpyridine) (P2VP). The hybrid micelles were successfully prepared by the rapid addition of acidic water to a binary solution of PCL_{34}-*b*-PEO_{114} and PCL_{32}-*b*-$P2VP_{52}$ diblock copolymers in N,N-dimethylformamide. These micelles were pH-responsive as result of the pH-dependent ionization of the P2VP block. The impact of pH on the self-assembly of the binary mixture of diblocks – thus on the composition, shape, size and surface properties of the micelles – was studied by a variety of experimental techniques, i.e., dynamic and static light scattering, transmission electron microscopy, Zeta potential, fluorescence spectroscopy and complement hemolytic 50 test.

Introduction

The unique capability of amphiphilic block copolymers to self-assemble in aqueous media, provide them with great potential in fields that require the availability of "intelligent",

e.g., stimuli-responsive, micelles. Whenever water (or an organic solvent) is selective towards one of the constitutive block, the copolymer chains can reversibly assemble into micellar aggregates, the covalent bonding of the blocks preventing macrophase separation from occurring. The more common morphology of polymeric micelles are core-shell structured nanospheres with an aggregated core surrounded and stabilized by a solvated shell.[1,2] The attention paid to the micellization of amphiphilic block copolymers is justified by their potential use as emulsifiers, detergents, paints and drug delivery systems.[3-8]

In order to increase the range of the available polymeric micelles and their properties, ABC triblock terpolymers and mixtures of AB + BC diblock copolymers were studied recently. Whenever the B block is the insoluble one, micelles with a mixed shell, thus consisting of two types of coronal blocks, A and C, are formed. If these blocks are miscible in water, the hybrid micelles are uniform, otherwise the shell is compartmentalized [9,10]. The immiscibility of the A and C blocks is of course detrimental to the micelle stability, and worse, it can prevent hybrid micelles from being formed from a mixture of AB and BC diblocks. This problem of hybridization was addressed by Munk et al.[11], who studied the micellization of polystyrene-*b*-poly(methacrylic acid) (PS-*b*-PMA) diblocks mixed with PMA-*b*-PS-*b*-PMA triblock copolymers. Hybridization can occur only when the transfer of unimers between the two types of micelles is possible. It is the reason why the diblock or triblock copolymers were dissolved in a dioxane (80 vol%)/water mixture for 48h, i.e. in a good solvent for PMA and a mild solvent for PS. The PS core of the individual micelles was thus solvated and allowed for micellar redistribution. It is only after mixing of the two populations of micelles and dialysis against buffered water that the hybrid micelles were kinetically frozen in. Procházka et al.[12-14] also prepared hybrid micellar systems with a polystyrene (PS) core and a mixed shell of PMA and poly(ethylene oxide) (PEO) blocks.

These two blocks are water soluble and fairly compatible with formation of interpolymer complexes at low pH.

Whenever the hydrophobic block of amphiphilic block copolymers is of a low glass transition temperature, unimer exchanges can lead to mixed micelles directly in water. Laschewsky et al.[15] prepared hybrid micelles in water by mixing micellar solutions of two poly(butyl acrylate)-*b*-poly(dimethylacrylamide) copolymers, PBA-*b*-PDMA, of different molecular weight. The key point is that the insoluble PBA block has a low glass transition temperature (Tg ~ -55°C), which makes the micelles dynamic. They also mixed micellar solutions of PBA-*b*-PDMA and PBA-*b*-poly(3-acrylamidopropyltrimethylammonium chloride). Aggregates with a monomodal size distribution were formed upon mixing in each type of mixture, indicating that mixed micelles were formed. Hybrid micelles of a mixture of di- and triblock copolymers were investigated by Gan et al.[16] Poly(ethyl acrylate), PEA, was chosen as the hydrophobic block consistent with a low Tg (Tg ~ -24°C). These authors investigated the micellization of binary mixtures of PEO-*b*-PEA and PEA-*b*-PEO-*b*-PEA in water. They concluded to the incorporation of the diblock chains into the rosette micelles formed by the triblock. Tsetanov et al.[17] prepared polymeric micelles with a mixed PEO/poly(2-hydroxyethyl methacrylate) (PHEMA) shell and a thermosensitive low Tg (~ -70°C) poly(propylene oxide), PPO, core, by mixing PEO-*b*-PPO-*b*-PEO and PHEMA-*b*-PPO-*b*-PHEMA triblock copolymers in water.

A few examples of three-component mixed micelles formed by one type of ABC triblock copolymers rather than by a mixture of AB and BC diblock copolymers were reported by Patrickios et al.[18-20] They studied the micellization of poly(2-(dimethylamino)ethyl methacrylate)-*b*-poly(methyl methacrylate)-*b*-poly(methacrylic acid), PDMAEMA-*b*-PMMA-*b*-PMAA, polyampholites in relation to pH. In contrast to PMMA which is hydrophobic, PDMAEMA and PMAA are hydrophilic and ionizable. Expectedly, a

PMMA core was surrounded by a binary shell of PDMAEMA and PMAA chains. These authors also investigated how PDMAEMA-*b*-PMMA-*b*-poly(hexa(ethylene glycol)methacrylate) triblock copolymers behave in water, the third PHEGMA block being a nonionic hydrophilic polymer.[21] It must be noted that a linear triblock copolymer, with three different constitutive blocks may exist as three topological isomers (ABC, ACB and BAC), which has a deep effect on the self-assembly in selective solvents.[22]

The purpose of this paper is to report on the preparation of pH-sensitive, stealthy and biodegradable hybrid micelles in a straightforward way, i.e., merely by mixing two diblock copolymers. Then, the pH dependent micellization of mixtures of PCL_{34}-*b*-PEO_{114} and PCL_{32}-*b*-$P2VP_{52}$ diblock copolymers is herein discussed. A few years ago, some of us reported the synthesis of PCL-*b*-PEO[23] and the preparation of nanocarriers therefrom.[24-26] In order to impart pH-responsiveness to these micelles, a PCL-*b*-P2VP copolymer was synthesized and hybrid micellization was investigated.

Experimental Section

Materials

Ethylene oxide was purchased from Messer. Styrene (99%, Aldrich), ε-caprolactone (99%, Aldrich) and 2-vinylpyridine (2VP, 97%, Aldrich) were purified by distillation over calcium hydride under reduced pressure. Toluene was distilled from sodium. All the other chemicals were used as received.

Synthesis of Diblock Copolymers

Synthesis of poly(ε-caprolactone)-block- poly(ethylene oxide)

The poly(ε-caprolactone)-*block*-poly(ethylene oxide) [PCL_{34}-b-PEO_{114}] was synthesized by living anionic ring-opening polymerization of ethylene oxide initiated by triethylene glycol-monomethylether in the presence of KOH, followed by the ε-caprolactone polymerization

initiated by the PEO chains end-capped by an aluminum alkoxide group as detailed elsewhere.[23] M_n(NMR) = 8900 g/mol, M_w/M_n = 1.15 ^{1}H NMR (400 MHz, $CDCl_3$), δ (TMS, ppm):1.38 (m, 2H, CH_2), 1.61-1.65 (m, 4H, CH_2), 2.29 (t, 2H, $COCH_2$), 3.36 (t, 3H, OCH_3, terminal), 3.62 (m, 4H, OCH_2CH_2), 4.05 (t, 2H, OCH_2).

Synthesis of poly(ε-caprolactone)-block- poly(2-vinylpyridine)

Poly(ε-caprolactone)-*block*- poly(2-vinylpyridine) [PCL_{32}-b-$P2VP_{52}$] was synthesized with a dual initiator (compound A, Scheme 1), as reported elsewhere.[27,28] Actually, the nitroxide mediated radical polymerization (NMP) of 2-vinylpyridine was combined with the coordinative ring-opening polymerization of ε-caprolactone. In a first step, α-alkoxyamine poly(ε-caprolactone) was synthesized as follows.[27] 1-hydroxy-2-phenyl-2-(2',2',6',6'-tetramethyl-1-piperidinyloxy)ethane (0.53 g, 1.8 mmol) (compound A in Scheme 1) was dried by azeotropic distillation of toluene and dissolved in dry toluene. Triethylaluminum (1.2 mL, 1.9 M in toluene) was added to the solution, and the mixture was stirred at room temperature for 1 h. ε-caprolactone (6.6 mL, 0.055 mol) was then added and reacted at 25°C for 17 h. A few drops of hydrochloric acid were added, the polymer was precipitated in cold heptane, dissolved again in toluene and precipitated in cold methanol as α-alkoxyamine PCL M_n(NMR) = 3700 g/mol, M_w/M_n = 1.5 ^{1}H NMR (400 MHz, $CDCl_3$), δ (TMS, ppm): 1.1 (s, 12H, CH_3), 1.38 (m, 2H, CH_2), 1.61-1.65 (m, 4H, CH_2), 2.29 (t, 2H, $COCH_2$), 4.05 (t, 2H, OCH_2), 7.25 (s, 5H, ArH). In the second step[29], the PCL macroinitiator (1g, 0.27 mmol) together with 4 mg of TEMPO (0.025 mmol) were added to 6 mL of 2-vinylpyridine (0.056 mol). After stirring at 130°C for 2h30, the reaction mixture was evaporated to dryness, dissolved in tetrahydrofuran and precipitated twice in heptane to give the purified PCL-*b*-P2VP copolymer. M_n(NMR)= 9200 g/mol, M_w/M_n = 1.33.^{1}H NMR (400 MHz, $CDCl_3$), δ (TMS, ppm): 1.36 (m, 1H, CH_2), 1.63 (m, 4H, CH_2), 1.79 (m, 2H, CH_2CH), 2.27 (m, 2H, CH_2CO), 4.04 (m, 2H, OCH_2), 6.4-7.3 (m, 3H, ArH), 8.0-8.3 (m, 1H, CHNC).

Micellization in water

Micelles of PCL_{32}-*b*-$P2VP_{52}$ and PCL_{34}-*b*-PEO_{114}, respectively were prepared by addition of water to the copolymer solutions in a water-miscible organic solvent. A solution of 20 mL of water (MilliQ) and 300 µL of hydrochloric acid (HCl, 1M) was rapidly added to 5 mL of a 1 wt% solution of each copolymer in N,N-dimethylformamide (DMF) under vigorous stirring for 2 h. The micellar solutions were then dialyzed against 1L of water for 15 h, through cellulose dialysis membranes (Spectrapor, cut-off 3500 Da).

The same procedure was used to prepare hybrid PCL-(P2VP/PEO) micelles. Then, the organic solution was a 50/50 (wt/wt) mixture of PCL_{32}-*b*-$P2VP_{52}$ and PCL_{34}-*b*-PEO_{114} copolymers in DMF. Hybrid micelles with protonated P2VP were collected. The deprotonated version was prepared by adding a solution of NaOH (1M) to the micellar solution followed by dialysis against water for 15 h.

Experimental techniques

Size Exclusion Chromatography

Size-exclusion chromatography (SEC) was carried out in tetrahydrofuran at 40 °C with a Waters 600 system equipped with a 410 refractive index detector (columns HP PL gel 5µm (10^5, 10^4, 10^3, 100 Å)) and calibrated with PS standards. The flow rate was 1mL/min.

Nuclear Magnetic Resonance Spectroscopy

^{1}H NMR (400 MHz) spectra were recorded at 25 °C with a Bruker AM 400 apparatus in $CDCl_3$ or D_2O.

Light Scattering

Dynamic light scattering measurements were performed on a Malvern CGS-3 equipped with a He-Ne laser (633 nm). A bath of filtered toluene surrounded the scattering cell, and the temperature was controlled at 25°C. Dynamic light scattering (DLS) measurements were performed at an angle of 90°. The polydispersity index (PDI) corresponds to the μ_2/Γ_1^2 ratio,

where μ_2 is the second cumulant and Γ_1 is the first cumulant. The DLS data were also analyzed by the CONTIN routine, a method which is based on a constraint inverse Laplace transformation of the data and which gives access to a size distribution histogram for the aggregates. Static light scattering (SLS) measurements were carried out at angles from 30 to 150°. The refractive index increment (dn/dc) was measured for each sample with a Mettler Toledo RE40D refractometer.

Fluorimetric Measurements

Fluorescence spectra of diblock copolymer micelles loaded with pyrene as a hydrophobic fluorescent probe were recorded with a spectrofluorimeter PERKIN ELMER LS50B. A stock solution of pyrene ($6\ 10^{-2}$ M) was prepared in acetone and stored at 5°C until use. When needed, this solution was added with deionized water until a pyrene concentration of $12\ 10^{-7}$ M. Acetone was then eliminated in vacuo at 60°C for 1 h. The acetone-free pyrene solution was mixed with micellar solutions of concentrations ranging from $1\ 10^{-3}$ to 5 g/L. These solutions were heated in an oven at 70°C for 4h, and stored overnight at room temperature. The final concentration of pyrene was $6\ 10^{-7}$ M, thus the solubility limit in water at 22°C. The fluorescence emission spectra were measured at the excitation wavelength (λexc) of 339 nm.

The critical micellar concentration (CMC) was determined from the dependence of the intensity of the first peak (I_1) of the emission spectrum at 375 nm versus the logarithm of the copolymer concentration.

Electrophoretic measurements

They were carried out with a Zetasizer 2000 Malvern Instruments and micellar solutions of 1 g/L at 20°C. The Zeta potential, ξ, was calculated from the electrophoretic mobility (U) on the basis of the relationship, $U = \epsilon\xi/\eta$, where η is the solution viscosity and ϵ is the dielectric constant.

Transmission Electron Microscopy

Transmission electron microscopy (TEM) was performed with a Philips CM-100 microscope. Samples were prepared by spin-coating a drop of micellar solution on a copper grid coated with Formvar.

Quartz Crystal Microbalance

A Q-Sense QCM-D S4 (Sweden) was used to measure masses adsorbed onto appropriately a gold coated quartz crystal. The adsorbed mass was calculated from a change in the overtone of the resonance frequency and the Sauerbrey equation[30]. After cleaning, the sensor and the O-ring were assembled in the QCM-D instrument, and Milli-Q water was injected into the sensor cell. The frequency was monitored until the baseline was stable. Water was replaced by a micellar solution, and the system was let to equilibrate. All the measurements were performed at a constant temperature of 25 °C.

Complement Activation

Complement activation was measured as the lytic capacity of a normal human serum (NHS) towards antibody-sensitized sheep erythrocytes after exposure to the micelles. Aliquots of NHS were incubated with increasing amounts of micelles. The amount of serum, required to haemolyse 50% of a constant number of sheep erythrocytes after exposure to the micelles, was determined ("CH50 units"). NHS was provided by the "Etablissement Français du Sang" (Angers, France) and stored as aliquots at – 80°C until use. Veronal-buffered saline containing 0.15 mM Ca^{2+} and 0.5 mM Mg^{2+} (VBS++) was prepared as reported elsewhere.[31] Firstly, sheep erythrocytes were sensitized by rabbit anti-sheep erythrocyte antibodies (Sérum hémolytique, Biomérieux, Marcy-l'Etoile, France) and diluted by the veronal-buffered saline at a final concentration of 2.10^9 cells/mL in VBS++. Increasing amounts of micellar solution were added to NHS diluted in VBS++ such that the final dilution of NHS in the mixture was 1/4 (v/v) in a final volume of 1 mL. After 1 h of incubation at 37°C under gentle agitation, the

suspension was diluted 1/25 (v/v) in VBS++, and aliquots of 8 different dilutions were added to a given volume of sensitized sheep erythrocytes. After 45 min of incubation at 37°C, the reaction mixture was centrifuged at 2000 rpm for 10 min. The absorption of the supernatant was measured at 414 nm with a microplate reader (Multiskan Anscent, Labsystems SA, Cergy-Pontoise, France) and compared to the data obtained with control serum in order to evaluate the amount of haemolysed erythrocytes. Positive and negative controls were carried out in each series of experiments in order to account for any difference in the hemoglobin response from a given erythrocyte preparation. Furthermore, corrections for particle light-scattering and spontaneous erythrocyte haemolysis were estimated by UV/VIS measurements with blanks containing only particles and only erythrocytes, respectively. In order to compare micelles of different average diameters, their surface area was calculated as follows: $S = 3 m/r\rho$, where S is the surface area [cm^2], m the weight [μg] in 1 mL nanosuspension, r the average radius [cm] determined by DLS, and ρ the volumetric mass [$\mu g/cm^3$] of the micelles estimated at 10^6 $\mu g/cm^3$.[32-34] The experimental data are the average of 3 independent experiments.

Results and Discussion

Synthesis of the Diblock Copolymers.

A typical poly(ε-caprolactone)-*block*-poly(ethylene oxide) diblock copolymer, [PCL_{34}-b-PEO_{114}] was synthesized as previously reported.[23] The targeted molecular weight (M_n), i.e., 5000 g/mol for the PEO block and 3900 g/mol for the PCL block, was reached by the appropriate control of the monomer to initiator ratios and the conversion of the monomer checked by ^{1}H-NMR. The polydispersity of this AB diblock copolymer was expected by quite narrow (1.15). The relative length of each constitutive block was selected for the micelles to be spherical (shorter PCL block) [35] and stealthy[36].

An original strategy was proposed for the synthesis of the PCL_{32}-b-$P2VP_{52}$ diblock copolymer based on a dual initiator that contained (i) a primary alcohol easily converted into an aluminum alkoxide, i.e., a well-known initiatior of the living ring-opening polymerization (ROP) of ε-caprolactone, (ii) an alkoxyamine, known for effective initiation of "controlled" nitroxide-mediated radical polymerization (NMP) of 2-vinylpyridine[29]. The structure of this dual initiator is shown in scheme 1 (compound A). This compound was synthesized according to a recipe reported elsewhere,[27,28] the expected structure being confirmed by ^{1}H NMR.

ε-caprolactone was polymerized by ROP in toluene at 25°C after reaction of the hydroxyl group of the dual initiator with triethylaluminum (Scheme 1).[27] The experimental conditions and the molecular characteristics of the alkoxyamine-terminated poly(ε-caprolactone) are listed in Table 1. After purification of this macromonomer by precipitation in heptane, the ^{1}H NMR spectrum (Figure 1a) showed the characteristic peaks of both the dual initiator at 1.1 ppm (methyl protons) and the PCL backbone at 4.1 ppm (-CH_2-O protons), at 2.29 ppm (methylene protons adjacent to the carbonyl) and at 1.65-1.38 ppm (methylene protons). M_n(NMR) of the PCL block was calculated according to eq.1 :

$$M_n(\text{NMR})_{PCL} = (12I_e/2I_g) \times 114 \qquad (1)$$

where I_e and I_g are the integral values of the peaks at 4.1 ppm (PCL) and 1.1 ppm (TEMPO end group); 114 is the molecular weight of the ε-CL monomer unit. M_n(NMR) is in good agreement with M_n(th), which also confirms the structure of the alkoxyamine-terminated PCL.

The poly(ε-caprolactone) end-capped by the alkoxyamine was used as a macroinitiator for the radical polymerization of 2-vinylpyridine with the purpose to prepare the PCL-*b*-P2VP copolymer (Scheme 1), under the conditions listed in Table 1. In agreement with Wohlrab et al.[29], the 2VP conversion was kept below 25% for the polydispersity of the P2VP block to be low ($M_w/M_n < 1.5$). The SEC profile of the accordingly prepared copolymer (Figure 2,

curve b) was monomodal (M_w/M_n = 1.33) and shifted towards lower elution volume compared to the alkoxyamine-terminated PCL macroinitiator (Figure 2, curve a). The ^{1}H NMR spectrum (Figure 1b) showed the peaks of the aromatic protons of the P2VP block in the 6.4-7.3 ppm range, except for the hydrogen atom adjacent to the nitrogen at 8.3 ppm. The signals for the aliphatic protons of both the P2VP block and the aliphatic protons of the PCL block overlapped each other (1.36-1.79 ppm). M_n(NMR) of the PCL-*b*-P2VP diblock was calculated by eq.2:

$$M_n(\text{NMR})_{\text{PCL-}b\text{-P2VP}} = (2I_h/I_e) \times \text{DP}_{\text{PCL}} \times 105 + M_{n\,\text{PCL}} \qquad (2)$$

where I_h and I_e are the integral values of the peaks at 8.3 ppm (P2VP) and 4.04 ppm (PCL); DP_{PCL} and $M_{n\,PCL}$ are the degree of polymerization and molecular weight of the alkoxyamine-terminated PCL (cfr supra), respectively and 105 is the molecular weight of the 2VP monomer unit. Again M_n(NMR) agrees well with M_n(th), which confirms that the expected PCL_{32}-*b*-$P2VP_{52}$ diblock was actually formed. The composition of this diblock is such that the degree of polymerization of the PCL block is similar to that one of the PCL_{34}-*b*-PEO_{114} copolymer.

Micellization of diblock copolymers

For the sake of comparison, micellization of the individual PCL_{34}-*b*-PEO_{114} and PCL_{32}-*b*-$P2VP_{52}$ diblock copolymers was studied in addition to that one of their 50/50 mixture. Micellization of PCL_{34}-*b*-PEO_{114} was triggered by the addition of acidified water (pH = 2) to a copolymer solution in DMF (1wt%), followed by dialysis against water (see Experimental Section). PCL being insoluble in water and PEO soluble in water at all pH's, micelles were formed with a hydrodynamic diameter of 46 nm (Table 2), as measured by DLS, and a narrow size distribution (Figure 3a). Micellization of the PCL_{32}-*b*-$P2VP_{52}$ copolymer was pH-dependent. For instance, whenever the P2VP block was uncharged (addition of water at pH = 7 to the DMF solution of the copolymer), flocculation occurred

during dialysis against water (pH = 7). In contrast, the partial protonation (theoretical protonation degree = 63%) of the P2VP block that occurred when acidified water (see Experimental Section) was added to the copolymer solution in DMF, resulted in micellization, and the micelles were stable even after dialysis against neutral water. Accordingly to DLS, these micelles of a hydrodynamic diameter of 25 nm coexisted with larger size aggregates (~215 nm) (Figure 3b). Hybrid micelles were prepared by addition of acidified water (pH = 2) to the copolymer mixture (50/50 wt/wt) dissolved in DMF (1wt%) (see Experimental Section). Figure 3c shows the characteristic size distribution reported by DLS. The profile is monomodal with an average hydrodynamic diameter of 41 nm and a narrow size distribution (Table 2), consistent with the formation of one population of micelles, which is a first hint for the formation of the hybrid micelles. Would each copolymer form micelles independently one of each other, the distribution would be the superposition of the profiles a and b in figure 3, which is not the case. A second evidence for the successful hybrid micellization can be found in the stability of the micelles against NaOH addition. Indeed, the micellar solution remained transparent (Figure 4c), in contrast to the solution of the micelles formed by the PCL-*b*-P2VP diblock copolymer that became cloudy (Figure 4a). The same observation was reported when the micelles formed by each copolymer were mixed (50/50 v/v) and added with NaOH solution (Figure 4b), because the P2VP block is no longer water-soluble when it is deprotonated, the PCL-*b*-P2VP copolymer flocculates at high pH, except when it is associated with the PCL-*b*-PEO copolymer into mixed micelles that resist increase in pH.

The micelles formed by each of the two diblock copolymers under consideration were observed by TEM. They were spherical with an average diameter of 30 nm for the PCL_{34}-*b*-PEO_{114} copolymer and 21 nm for the PCL_{32}-*b*-$P2VP_{52}$ diblock. The hybrid micelles with protonated P2VP were also spherical with an average diameter of 24 nm (Figure 5a).

That the PCL-*b*-PEO micelles consisted of a neutral PEO shell was confirmed by a very low ξ potential (Table 2), whereas the highly positive ξ potential of the PCL-*b*-P2VP micelles was consistent with a shell of protonated P2VP. In line with a binary composition, the PCL core of the mixed micelles was surrounded by a mixture of positively charged P2VP and neutral PEO (Scheme 2), as assessed by a ξ potential in between the values reported for each of the constitutive diblocks (Table 2).

Micelle formation was monitored by fluorimetry in the presence of pyrene as a hydrophobic fluorescent probe. Because its fluorescence is sensitive to the philicity of the microenvironment, pyrene can probe micellization in water, and the critical micellar concentration (CMC) can be determined, as result of the pyrene incorporation into the hydrophobic core of the micelles. Figure 6 shows that the intensity (I_1) of the first emission peak of pyrene at 375 nm depends on the copolymer concentration. The CMC, that corresponds to the crossover point at low concentration, was 2.2 10^{-5} mol/L for the PCL_{34}-*b*-PEO_{114} micelles (Figure 6a) and 1.9 10^{-5} mol/L for the PCL_{32}-*b*-$P2VP_{52}$ micelles (Figure 6b). Only one CMC was noted for the hybrid micelles at a concentration of 9.8 10^{-6} g/mol (Figure 6c), which is in favor of the hybridization rather than a mixture of two types one-component micelles.

The effect of the protonation of the P2VP block on the hybrid micellization was studied, by changing the amount of HCl used in the micelle preparation. Table 3 shows that when this amount was decreased, the hydrodynamic diameter of the micelles also decreased (samples 1a, b, and c, in Table 3) as result of a lower degree of protonation, and thus a lower stretching of the P2VP chains in the micellar shell. In parallel, the ξ potential decreased with decreasing amount of HCl. The influence of the pH of water used in dialysis was also examined. When the micelles were dialyzed against neutral water, proton transfer occurred at the expense of the P2VP protonation, such that the actual degree of protonation was smaller

than the theoretical one. The micelles prepared with an excess of HCl compared to the 2VP units (sample 2a, in Table 3) were dialyzed against water at pH 3 instead of neutral water. The diameter and the ξ potential of the hybrid micelles were then the highest as the protonation of the P2VP block should be.

In order to highlight the pH-sensitivity of the hybrid micelles, the protonated version was neutralized by addition of a NaOH solution (10^{-2}M), followed again by dialysis against water, with the purpose to make the P2VP block insoluble in water. The hydrodynamic diameter of the neutralized micelles was 49 nm as measured by DLS (Table 2), and the size distribution was very narrow. Whatever the amount of HCl used in the original micellization step, the micelles after neutralization by NaOH had the same hydrodynamic diameter (Table 3). Moreover, when micellization was triggered by addition of water (pH = 7) to the DMF solution (sample 1d, in Table 3), D_h of the micelles was identical to the case where water at low pH was used followed by neutralization (samples 1a, b, c, in Table 3). When the P2VP block was deprotonated, the size of the micelles thus increased from 41 to 49 nm. TEM observations confirmed this evolution by showing spheres with a larger diameter of 28 nm (Figure 5c). The ξ potential was close to zero, in line with the deprotonation of P2VP and collapse, leaving a solvated shell of neutral PEO chains (Table 2). These hybrid micelles were further characterized by static light scattering (SLS) in order to account for the aforementioned size data. SLS was carried out in the concentration range of 1 g/L ≤ c ≤ 5 g/L. The SLS data are reported in Table 4. The weight-average molecular weight of the micelles with protonated P2VP was determined by plotting the experimental data in a Zimm plot: $M_{w,micelle}$ = 4.2 10^5 g/mol. An aggregation number of 37 was calculated as $M_{w,micelle}$ / [$M_{w,PCL\text{-}b\text{-}PEO}$ + $M_{w,PCL\text{-}b\text{-}P2VP}$)/2]). A z-average radius of gyration, R_g = 14 nm, was also extracted and compared to R_h determined by DLS. The R_g/R_h ratio was 0.85, thus close to the theoretical value (0.776) for a hard sphere, consistent with micelles with a core-shell structure.[34,35] When

the P2VP block was deprotonated, a higher weight-average molecular weight was found for the micelles ($M_{w,micelle}$ = 1.26 10^6 g/mol) and thus a larger aggregation number, Nagg = 111. Clearly, the deprotonation of the P2VP triggers for the reorganization of the micelles that increases their average aggregation number and hydrodynamic diameter. Conversion of polycationic P2VP hydrated in the shell to insoluble neutral chains results in a higher hydrophobic content which is deleterious to the stability of the micelles (loss of an electrostatic repulsion barrier). The micellar reorganization occurs for the steric stabilization by the solvated PEO blocks to be most effective (Scheme 2).

The hybrid micelles were also analyzed by ^{1}H NMR in D_2O (Figure 7). The protons of P2VP were expectedly observed when the chains were protonated, thus solvated and mobile (Figure 7a). In contrast, no resonances was detected for the non protonated P2VP blocks, that were collapsed and thus of a restricted mobility (Figure 7b). A symmetric singlet at 3.6 ppm was the signature of the PEO blocks, whatever the pH at which the micelles were formed in agreement with the non sensitivity of PEO to pH. Surprisingly enough, the protons of PCL were observed at 4.05 ppm and 1.1-2.29 ppm although PCL was part of the micellar core. This observation strongly suggests that the PCL core is not in the glassy state and that the chains are mobile enough for the resonance of the protons to be detected, [37] and the micelles to reorganize themselves upon deprotonation of the P2VP blocks.

An additional evidence of the responsiveness of the micelles to pH was found in an adsorption experiment carried out with a quartz crystal microbalance (QCM). This equipment is sensitive to mass changes, which are monitored as changes in the resonance frequency of a quartz crystal. Basically, the interaction of the hybrid micelles with a negatively charged QCM sensor was probed by QCM. A commercially available gold sensor was first coated [38] by positively charged polyethyleneimine, followed by the deposition of a polystyrenesulfonate (PSS) layer, so making the surface of the sensor negatively charged

When protonated hybrid micelles were in contact with the surface modified sensor, a rapid increase in mass was observed (ca. 1812 ng/cm^2) as result of micelles uptake by electrostatic interaction (Figure 8a). From the weight-average molecular weight of the micelles (M_w,micelles = 4.2 10^5 g/mol, Table 4), it was found that 4.3 10^{-12} mol of micelles were adsorbed per cm^2 of surface area. Conversely, the mass of the sensor changed only slightly (208 ng/cm^2) for the hybrid micelles with unprotonated P2VP (M_w,micelles = 1.26 10^6 g/mol) (Figure 8b). Actually, 1.65 10^{-13} mol of micelles were adsorbed per cm^2 of surface area, thus 26 times less compared to the micelles with protonated P2VP, in agreement with a deep influence of pH on the structure and surface properties of these micelles.

The pH-dependency of the electrostatic interactions of the hybrid micelles with a negatively charged surface is evidence that positive charges are available at the outer periphery of the protonated micelles, thus that the charged P2VP blocks protrude the PEO shell. Would they be buried within the shell, these interactions could not occur as illustrated by protonated micelles formed by the PS_{200}-*b*-$P2VP_{140}$-*b*-PEO_{590} triblock copolymer (D_h = 89.8 nm, ζ = 10.8±1.3 mV, N_{agg} = 113), discussed elsewhere by Gohy et al.[39]. The cationic P2VP being the central block, the positive charges cannot be exposed at the surface of the micelles, M_w,micelles = 7.6 10^6 g/mol, whose the adsorption onto a negatively charged surface is unfavorable. Indeed, a mass increase of 1329 ng/cm^2 was observed that corresponds to the adsorption of 1.7 10^{-13} mol of micelles per cm^2 of surface area. This adsorbed amount is expectedly very close to that one observed for the unprotonated hybrid micelles. This indicates that in the case of the hybrid micelles the protonated P2VP chains emerge out of the PEO shell, exhibiting accessible positive charges at the outer periphery and allowing to strongly modulate the surface properties of the micelles by simply playing with the pH.

Complement activation

The ability of the hybrid micelles with a PEO shell to repel proteins was also investigated by the so-called CH50 test, that quantifies the adsorption of human serum proteins (complement proteins) on the micelles.[32-34] Indeed, because of a small size, micelles are potential carriers for hydrophobic drugs, that can be directly injected in the bloodstream.[3,4,6,7] However, the activation of the complement system, one of the major mechanisms by which the immune system eliminates foreign bodies, can result in the particle opsonisation. The first step of this process is the adsorption of the C3 complement protein to the particle surface. Nevertheless, the PEO coating of small size particles (such as micelles) proved efficiency in restricting the proteins adsorption.[36,40,41] Such particles, designated as stealthy, are highly desirable in case of long-circulating drug carriers systems.

The activation of the complement system by a foreign body can be quantified in vitro by the CH50 test that consists in using sensitized sheep erythrocytes prone to lysis when exposed to proteins of human serum. As a result, the released hemoglobin can be used as a dye in a colorimetric titration. The CH50 unit is the concentration per mL of serum of complement units able to cause 50% haemolysis of a fixed volume of the sheep red cells after exposure to the micelles. So, a less extended adsorption of the proteins onto the micelles results in a more extended lysis of the sensitized sheep erythrocytes. The experimental results are expressed as the percentage of the CH50 unit consumed as a function of the micellar surface.

As a rule, whatever the tested micelles, Figure 9 shows the expected tendency of the CH50 consumption to increase with the amount of micelles in the serum, i.e., with the total surface area that interacts with the proteins. As reported elsewhere,[42] PEO-*b*-PCL micelles were stealthy as assessed by a low CH50 consumption (curve a, in Figure 9). In contrast, the positively charged surface of protonated PCL-*b*-P2VP micelles strongly activated the

complement system (curve b, in Figure 9), as result of electrostatic interactions with negatively-charged proteins.[43]

Compared to the PCL_{34}-*b*-PEO_{114} and protonated PCL_{32}-*b*-$P2VP_{52}$ micelles, the hybrid micelles under consideration in this study showed an intermediate CH50 consumption when protonated (curves c in Figure 9). This is merely the consequence of the mixed composition of the shell, the deleterious impact of cationic P2VP being attenuated by the favorable contribution of PEO to stealthiness, and, vice-versa, the beneficial effect of PEO is counterbalanced by the negative impact of charged P2VP. Quite interestingly, deprotonation of the hybrid micelles is enough for them to compete effectively PEO-b-PCL micelles as emphasized by a similar low CH50 consumption (curves a and d, in Figure 9). Then, only PEO is exposed to the proteins containing medium. These biological experiments confirm, if necessary, the crucial impact of the pH-dependent surface properties of the mixed micelles prepared in this study. pH is quite an easily manipulated stimulus that decides the fate of the supramolecular assembly of the copolymers and the final properties of the accordingly formed micelles.

Conclusions

A novel PCL_{32}-*b*-$P2VP_{52}$ diblock copolymer was synthesized by combining living ROP and controlled radical polymerization (NMP) by using a dual initiator. Micellization of this diblock copolymer with a protonated P2VP block was studied and compared to a more conventional PCL_{34}-*b*-PEO_{114} amphiphilic diblock. Micellization of a mixture of these two diblocks is a straightforward way to hybrid micelles that consist of a PCL core surrounded by a mixed PEO/P2VP shell out of which the stretched cationic P2VP block emerges at the outer periphery. Quite interestingly, these micelles are pH-sensitive as illustrated by their pH-driven reorganization, which changes not only the size but more importantly the surface properties of

the micelles. At low pH, the micelles are positively charged and prone to interact with negative surfaces. At high pH, the surface charges of the micelles do not persist, the PEO blocks are exposed to the external medium and stealthiness is then key feature of the mixed micelles that have potential as long circulating drug carriers.

Acknowledgement

The authors are grateful to the "Services Fédéraux des Affaires Scientifiques, Techniques et Culturelles" in the frame of the "Pôles d'Attraction Interuniversitaires: VI-27". K.V.B. is grateful to the "Fonds pour la Formation à la Recherche dans l'Industrie et dans l'Agriculture" (FRIA) for a fellowship. C.A.F. is Research Associate of the FRS-FNRS.

References

[1] G. Riess, Progress in Polymer Science 28 (2003) 1107.
[2] J.-F. Gohy, Advances in Polymer Science 190 (2005) 65.
[3] G.S. Kwon, T. Okano, Advanced Drug Delivery Reviews 21 (1996) 107.
[4] M.C. Jones, J.C. Leroux, European Journal of Pharmaceutics and Biopharmaceutics 48 (1999) 101.
[5] P. Alexandridis, B. Lindman, Editors, Amphiphilic Block Copolymers: Self-Assembly and Applications, 2000.
[6] K. Kataoka, A. Harada, Y. Nagasaki, Advanced Drug Delivery Reviews 47 (2001) 113.
[7] V.P. Torchilin, Pharmaceutical Research 24 (2007) 1.
[8] C. Jerome, P. Lecomte, Advanced Drug Delivery Reviews 60 (2008) 1056.
[9] I.K. Voets, A. de Keizer, P. de Waard, P.M. Frederik, P.H.H. Bomans, H. Schmalz, A. Walther, S.M. King, F.A.M. Leermakers, M.A. Cohen Stuart, Angewandte Chemie, International Edition 45 (2006) 6673.
[10] R. Erhardt, M. Zhang, A. Boeker, H. Zettl, C. Abetz, P. Frederik, G. Krausch, V. Abetz, A.H.E. Mueller, Journal of the American Chemical Society 125 (2003) 3260.
[11] M. Tian, A. Qin, C. Ramireddy, S.E. Webber, P. Munk, Z. Tuzar, K. Prochazka, Langmuir 9 (1993) 1741.
[12] M. Stepanek, K. Podhajecka, E. Tesarova, K. Prochazka, Z. Tuzar, W. Brown, Langmuir 17 (2001) 4240.
[13] K. Podhajecka, M. Stepanek, K. Prochazka, W. Brown, Langmuir 17 (2001) 4245.
[14] P. Matejicek, J. Humpolickova, K. Prochazka, Z. Tuzar, M. Spirkova, M. Hof, S.E. Webber, Journal of Physical Chemistry B 107 (2003) 8232.
[15] S. Garnier, A. Laschewsky, Macromolecules 38 (2005) 7580.
[16] S. Dai, P. Ravi, C.Y. Leong, K.C. Tam, L.H. Gan, Langmuir 20 (2004) 1597.
[17] P. Petrov, M. Bozukov, M. Burkhardt, S. Muthukrishnan, A.H.E. Mueller, C.B. Tsvetanov, Journal of Materials Chemistry 16 (2006) 2192.
[18] C.S. Patrickios, W.R. Hertler, N.L. Abbott, T.A. Hatton, Macromolecules 27 (1994) 930.

[19] W.-Y. Chen, P. Alexandridis, C.-K. Su, C.S. Patrickios, W.R. Hertler, T.A. Hatton, Macromolecules 28 (1995) 8604.
[20] C.S. Patrickios, A.B. Lowe, S.P. Armes, N.C. Billingham, Journal of Polymer Science, Part A: Polymer Chemistry 36 (1998) 617.
[21] A.I. Triftaridou, M. Vamvakaki, C.S. Patrickios, Polymer 43 (2002) 2921.
[22] C.A. Fustin, V. Abetz, J.F. Gohy, European Physical Journal E: Soft Matter 16 (2005) 291.
[23] P. Vangeyte, R. Jerome, Journal of Polymer Science, Part A: Polymer Chemistry 42 (2004) 1132.
[24] H.M. Aliabadi, A. Mahmud, A.D. Sharifabadi, A. Lavasanifar, Journal of Controlled Release 104 (2005) 301.
[25] X. Shuai, H. Ai, N. Nasongkla, S. Kim, J. Gao, Journal of Controlled Release 98 (2004) 415.
[26] E.K. Park, S.Y. Kim, S.B. Lee, Y.M. Lee, Journal of Controlled Release 109 (2005) 158.
[27] C.J. Hawker, J.L. Hedrick, E.E. Malmstroem, M. Trollss, D. Mecerreyes, G. Moineau, P. Dubois, R. Jerome, Macromolecules 31 (1998) 213.
[28] D.J. Gravert, K.D. Janda, Tetrahedron Letters 39 (1998) 1513.
[29] S. Wohlrab, D. Kuckling, Journal of Polymer Science, Part A: Polymer Chemistry 39 (2001) 3797.
[30] G. Sauerbrey, Zeitschrift fuer Physik 155 (1959) 206.
[31] E.A. Kabat, M.M. Mayer, Experimental Immunochemistry. 2nd ed, 1961.
[32] M. Vittaz, D. Bazile, G. Spenlehauer, T. Verrecchia, M. Veillard, F. Puisieux, D. Labarre, Biomaterials 17 (1996) 1575.
[33] C. Passirani, G. Barratt, J.-P. Devissaguet, D. Labarre, Life Sciences 62 (1998) 775.
[34] C. Passirani, J.-P. Benoit, Complement activation by injectable colloidal drug carriers, 2005.
[35] P. Vangeyte, B. Leyh, M. Heinrich, J. Grandjean, C. Bourgaux, R. Jerome, Langmuir 20 (2004) 8442.
[36] R. Gref, M. Luck, P. Quellec, M. Marchand, E. Dellacherie, S. Harnisch, T. Blunk, R.H. Muller, Colloids and Surfaces, B: Biointerfaces 18 (2000) 301.
[37] T. Riley, S. Stolnik, C.R. Heald, C.D. Xiong, M.C. Garnett, L. Illum, S.S. Davis, S.C. Purkiss, R.J. Barlow, P.R. Gellert, Langmuir 17 (2001) 3168.
[38] S. Disawal, J. Qiu, B.B. Elmore, Y.M. Lvov, Colloids and Surfaces, B: Biointerfaces 32 (2003) 145.
[39] J.-F. Gohy, N. Willet, S.K. Varshney, J.-X. Zhang, R. Jerome, e-Polymers (2002) Paper No 35.
[40] P. Vermette, L. Meagher, Colloids and Surfaces B: Biointerfaces 28 (2003) 153.
[41] J.H. Lee, S.H. Oh, Journal of Biomedical Materials Research 60 (2002) 44.
[42] J. Rieger, C. Passirani, J.-P. Benoit, K. Van Butsele, R. Jerome, C. Jerome, Advanced Functional Materials 16 (2006) 1506.
[43] A. Vonarbourg, C. Passirani, P. Saulnier, J.-P. Benoit, Biomaterials 27 (2006) 4356.

Scheme 1

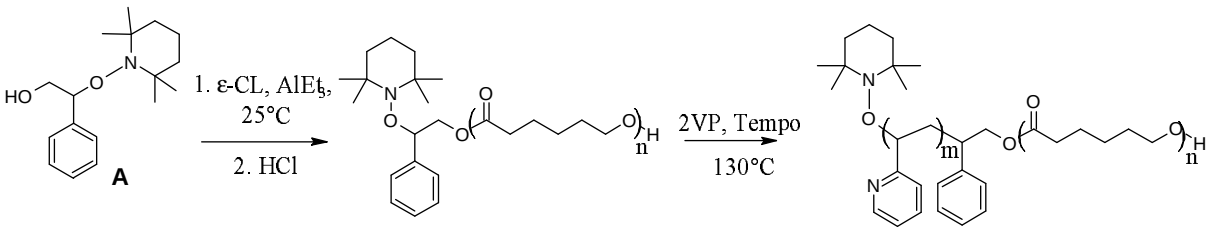

Scheme 2

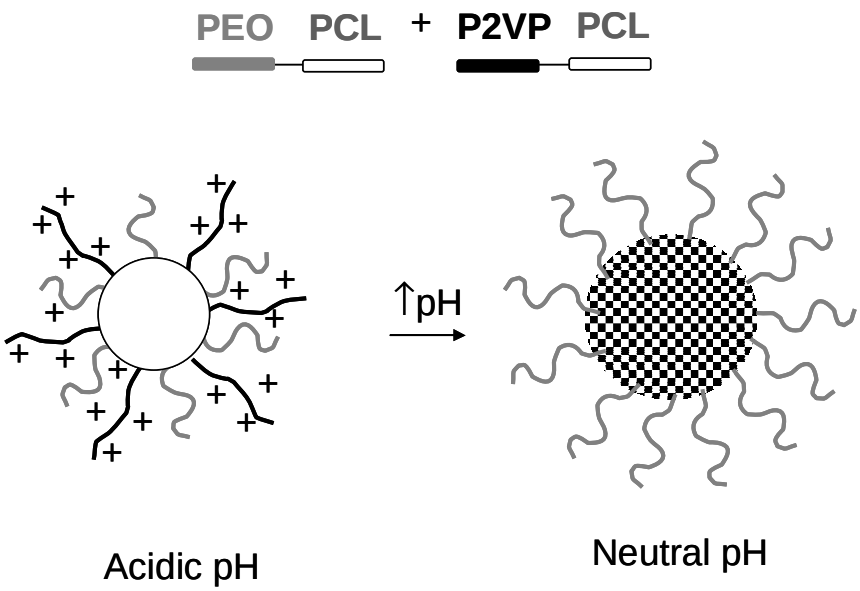

Table 1. Synthesis and characterization of alkoxyamine-terminated PCL[a] and PCL_{32}-*b*-$P2VP_{52}$ copolymer [b].

sample	$[M]_0/[I]_0$	Conv (%)	M_n(th)	M_n(exp)[e]	M_w/M_n (SEC)
Alkoxyamine-terminated PCL	31	100	3500 [c]	3700	1.50
PCL-*b*-P2VP	224	25	9600 [d]	9200	1.33

[a] ε-CL was polymerized by ring opening polymerization in toluene at 25°C. [b] 2VP was polymerized by nitroxide mediated radical polymerization in bulk at 130°C [c] M_n(th) = ($[M]_0/[I]_0$) x conversion x 114, where $[M]_0$ and $[I]_0$ are the initial molar concentrations of ε-CL and the dual initiator, respectively; 114 is the molecular weight of ε-CL.[d] M_n(th) = [($[M]_0/[I]_0$) x conversion x 105] + 3700, where $[M]_0$ and $[I]_0$ are the initial molar concentrations of 2VP and the alkoxyamine-terminated PCL, respectively; 105 is the molecular weight of 2VP; 3700 is the molecular weight of the alkoxyamine-terminated PCL. [e] calculated by ^{1}H NMR according to eqs. 1 and 2, respectively.

Table 2. DLS, ξ potential and fluorescence data for the micelles formed by the PCL_{34}-*b*-PEO_{114} diblock, the PCL_{32}-*b*-$P2VP_{52}$ diblock and a 50/50 (wt/wt) mixture of the two copolymers (c = 1 g/L).

sample	H^+(th) (%)[a]	Dh (nm)[b]	μ_2/Γ^2 [c]	ξ potential (mV)[d]	Cmc (g/mol)[e]
PCL-b-PEO	-	46	0.20	7 ± 5	$2.2\ 10^{-5}$
PCL-b-P2VP	63	25/215	0.25	65 ± 5	$1.9\ 10^{-5}$
Hybrid	Max	41	0.11	35± 5	$9.8\ 10^{-6}$
Hybrid	-	49	0.078	7± 5	-

[a] Theoretical degree of P2VP protonation. [b] Hydrodynamic diameter determined by a CONTIN analysis of the DLS data. [c] Polydispersity index determined by a cumulant analysis of the DLS data. [d] Zeta potential determined by electrophoretic measurement. [e] Critical micellar concentration determined by fluorometry measurements.

Table 3. Influence of the degree of protonation on the hybrid micelles (c = 1 g/L): DLS and ξ potential data.

sample	HCl (μL)[a]	pH for dialysis	Dh (nm)[b]	μ_2/Γ^2 [c]	ξ potential (mV)[d]	Dh (nm) after NaOH addition[b]	μ_2/Γ^2 [c]
1a	300	neutral	41	0.112	35 ± 5	49	0.078
1b	150	neutral	36	0.165	30 ± 5	49	0.08
1c	75	neutral	33	0.128	25± 5	49	0.08
1d	0	neutral	49	0.160	2± 5	/	/
2a	300	3	45	0.108	40± 5	49	0.09

[a]HCl volume added to the 20 mL of water to be added to the copolymers solution in DMF. [b] Hydrodynamic diameter determined by a CONTIN analysis of the DLS data. [c]Polydispersity index determined by a cumulant analysis of the DLS data. [d]Zeta potential determined by electrophoretic measurement.

Table 4. DLS and SLS data for the hybrid micelles (c = 1 g/L).

sample	H^+(th) (%)[a]	Dh (nm)[b]	μ_2/Γ^{2} [c]	Mw[d]	Nagg[e]	Rg[f]	Rg/Rh
Hybrid	31.5	33	0.128	$4.2\ 10^5$	37	14	0.85
Hybrid	/	49	0.08	$1.26\ 10^6$	111	22	0.9

[a] Theoretical degree of P2VP protonation. [b] Hydrodynamic diameter determined by by a CONTIN analysis of the DLS data. [c] Polydispersity index determined by a cumulant analysis of the DLS data. [d] Molecular weight of the micelles determined by SLS. [e] Aggregation number of the micelles, Nagg = (Nagg = $2M_{w,micelle}$ / ($M_{w,PCL\text{-}b\text{-}PEO}$ + $M_{w,PCL\text{-}b\text{-}P2VP}$)). [f]z-average radius of gyration determined by SLS.

Figure captions

Figure 1. ^{1}H NMR spectrum of (a) the alkoxyamine-terminated PCL and (b) the PCL_{32}-*b*-$P2VP_{52}$ copolymer.

Figure 2. SEC curves for (a) alkoxyamine-terminated PCL, (b) PCL_{32}-*b*-$P2VP_{52}$ copolymer.

Figure 3. CONTIN distribution function of the diameter of the (a) PCL_{34}-*b*-PEO_{114} micelles, (b) PCL_{32}-*b*-$P2VP_{52}$ micelles, (c) PCL-(PEO/P2VP) hybrid micelles with protonated P2VP in water (c = 1 g/L, $\theta = 90°$).

Figure 4. Micellar stability against the addition of NaOH on (a) PCL_{32}-*b*-$P2VP_{52}$ micelles, (b) the 50/50 (v/v) mixture of PCL_{34}-*b*-PEO_{114} and PCL_{32}-*b*-$P2VP_{52}$ micellar solution, (c) the PCL-(PEO/P2VP) hybrid micelles with protonated P2VP.

Figure 5. TEM micrographs of the PCL-(PEO/P2VP) hybrid micelles in water with (a) protonated P2VP, (b) deprotonated P2VP.

Figure 6. Concentration dependence of emission intensity (I_1) at 375 nm of (a) PCL_{34}-*b*-PEO_{114} micelles, (b) PCL_{32}-*b*-$P2VP_{52}$ micelles, (c) the PCL-(PEO/P2VP) hybrid micelles with protonated P2VP.

Figure 7. ^{1}H NMR spectra of the PCL-(PEO/P2VP) hybrid micelles in D2O with (a) protonated P2VP, (b) deprotonated P2VP.

Figure 8. Time dependence of the mass uptake monitored by QCM for the adsorption, onto a negatively charged quartz crystal of (a) PCL-(PEO/P2VP) hybrid micelles with protonated P2VP, (b) PCL-(PEO/P2VP) hybrid micelle with unprotonated P2VP, (c) PS-*b*-P2VP-*b*-PEO micelles with protonated P2VP.

Figure 9. CH50 consumption versus the micellar surface area of (a) PCL_{34}-*b*-PEO_{114} micelles, (b) PCL_{32}-*b*-$P2VP_{52}$ micelles, (c) PCL-(PEO/P2VP) hybrid micelles with protonated P2VP, (d) PCL-(PEO/P2VP) hybrid micelles with unprotonated P2VP.

Figure 1

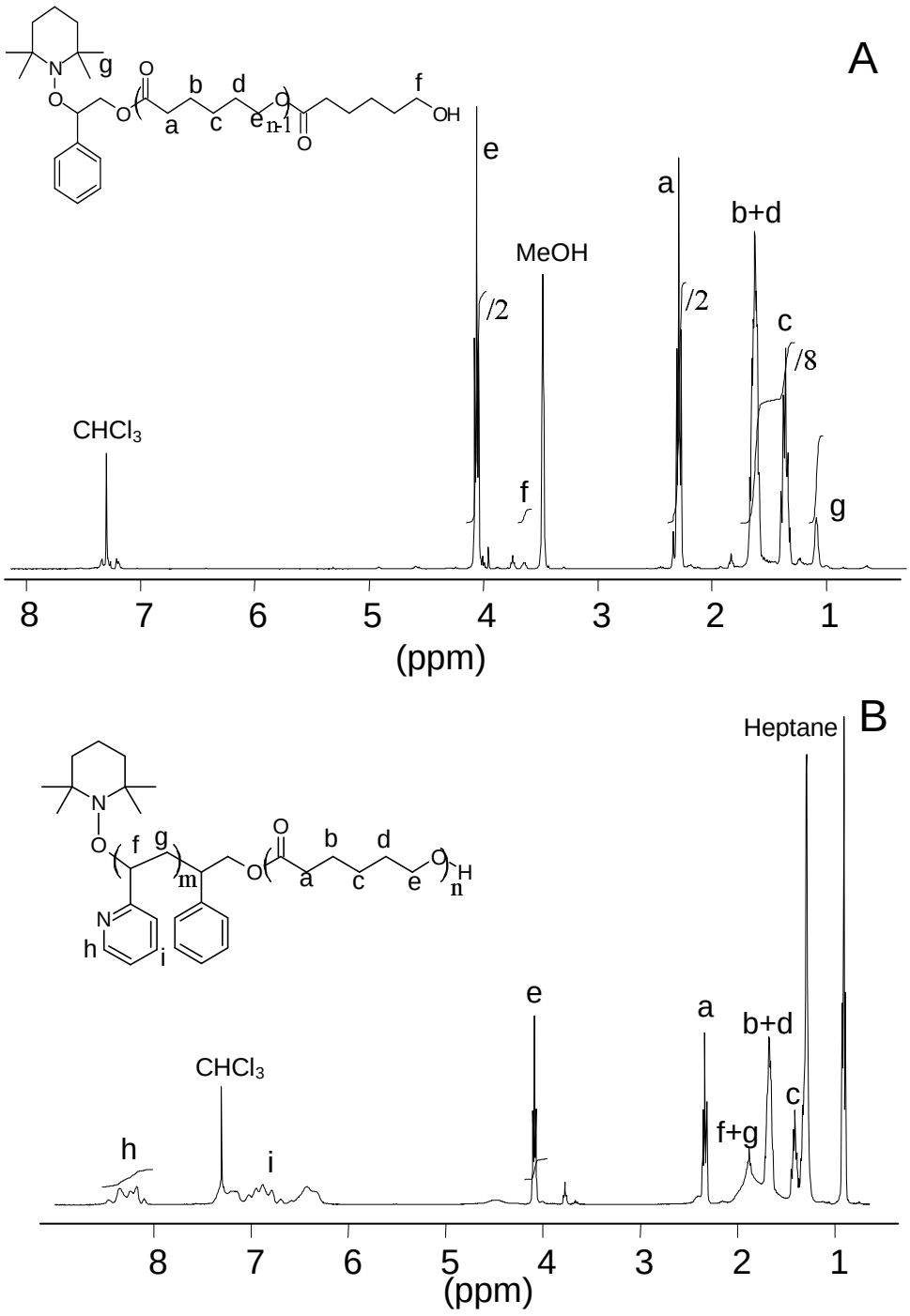
A
g
O
b
d
f
OH
N
O
O
a
c
e
n-1
O
e
a
b+d
MeOH
/2
/2
c
/8
CHCl3
f
g
8
7
6
5
4
3
2
1
(ppm)
B
Heptane
N
O
f
g
m
O
O
b
d
O
H
a
c
e
n
N
h
i
e
a
b+d
CHCl3
c
f+g
h
i
8
7
6
5
4
3
2
1
(ppm)

Figure 2

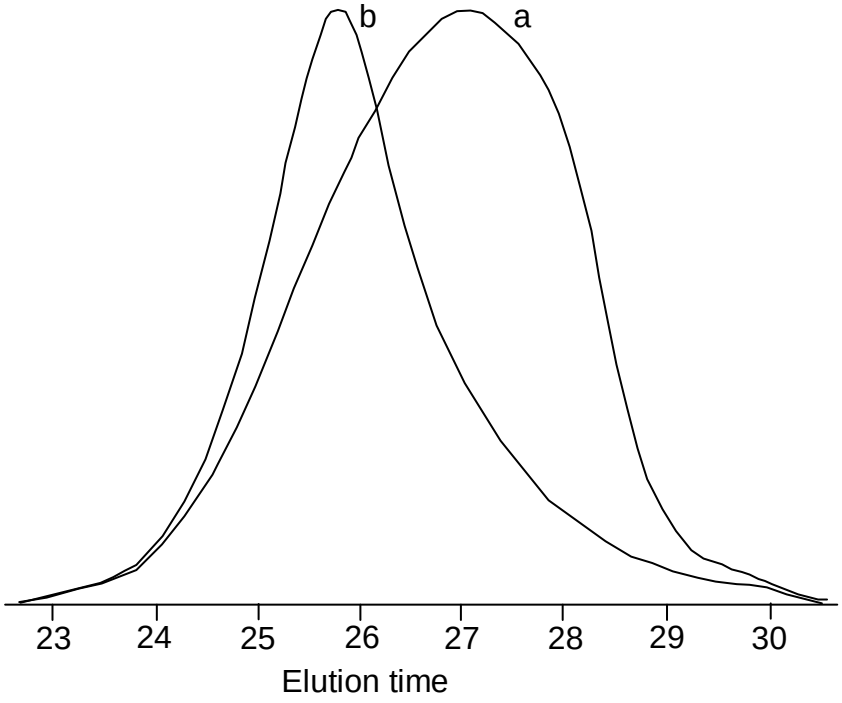

Figure 3

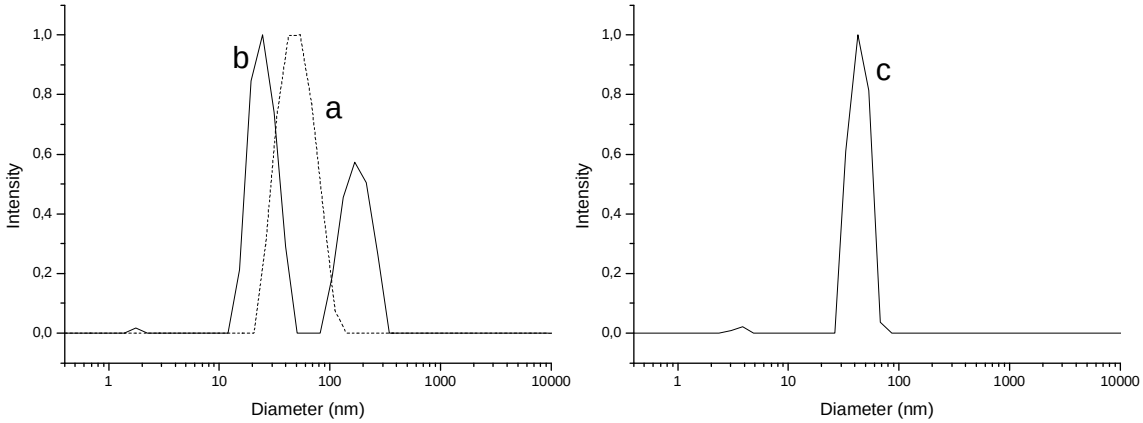

Figure 4

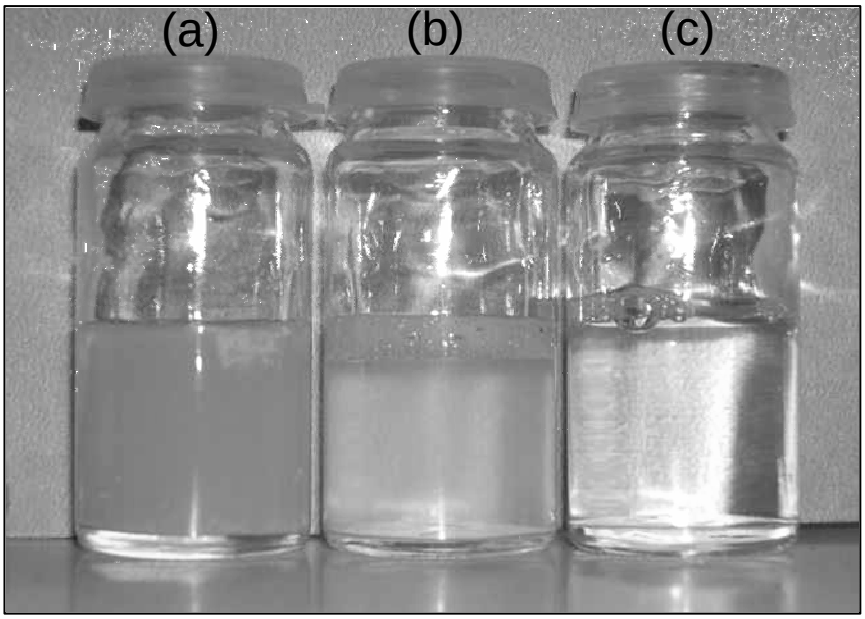

Figure 5A

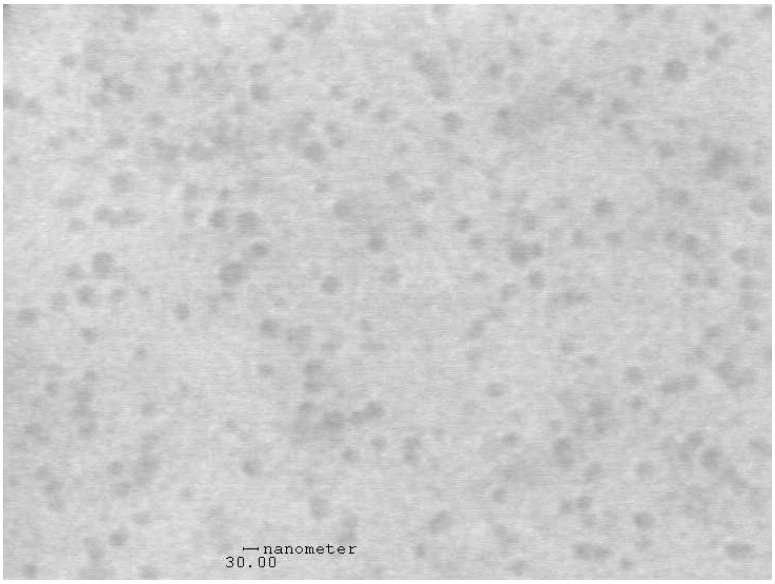

Figure 5B

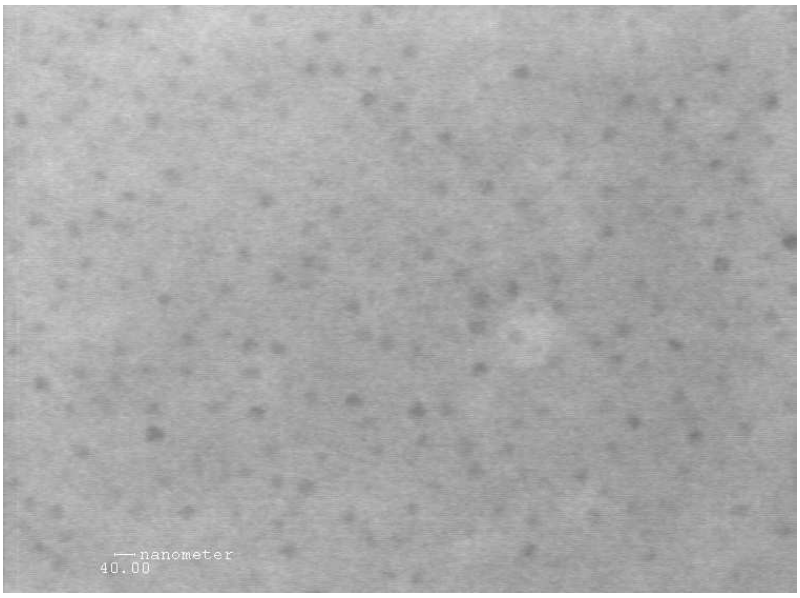

Figure 6

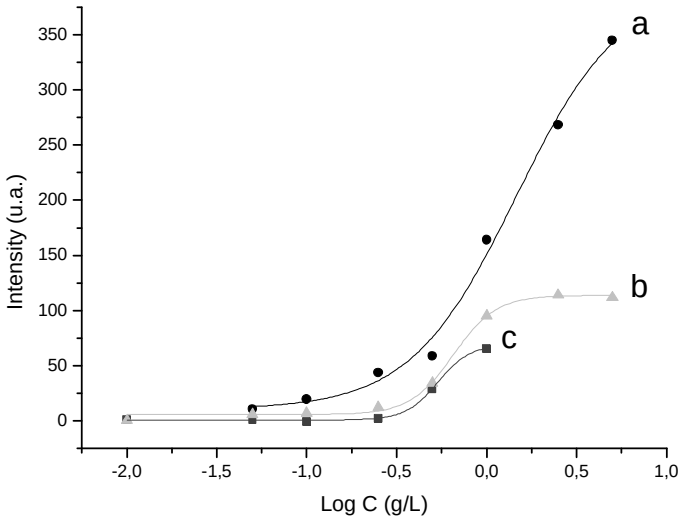
Intensity (u.a.)
Log C (g/L)
a
b
c
350
300
250
200
150
100
50
0
-2,0
-1,5
-1,0
-0,5
0,0
0,5
1,0

Figure 7

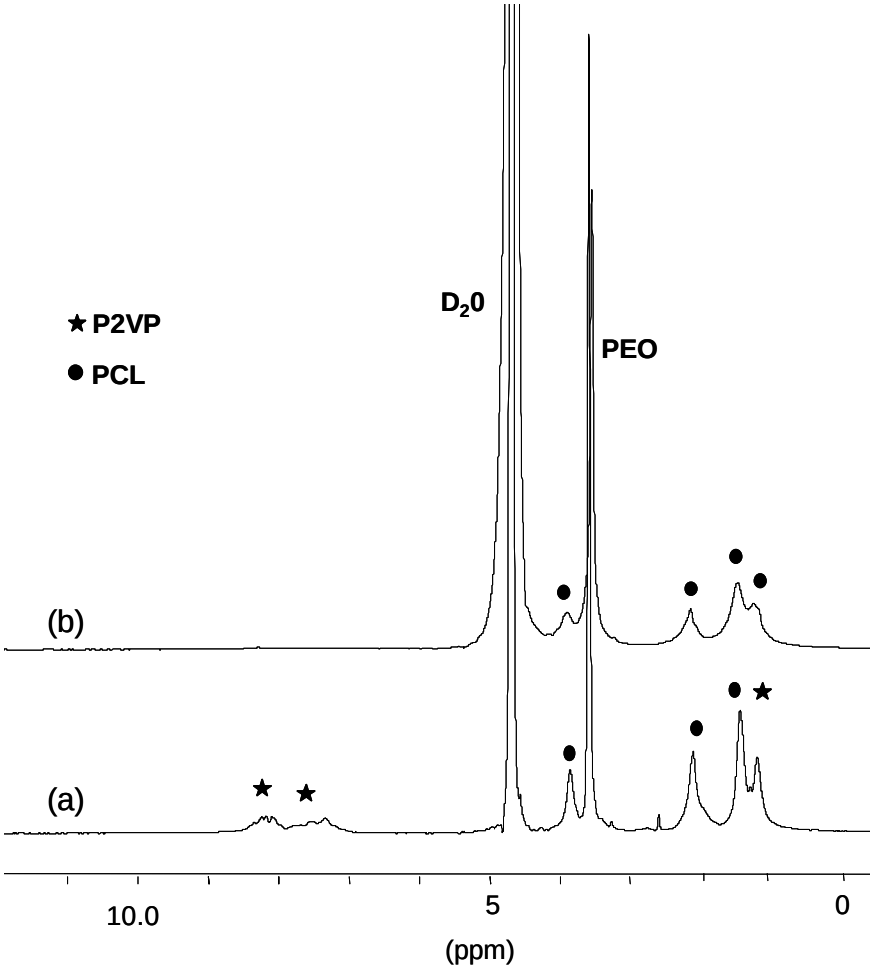

Figure 8

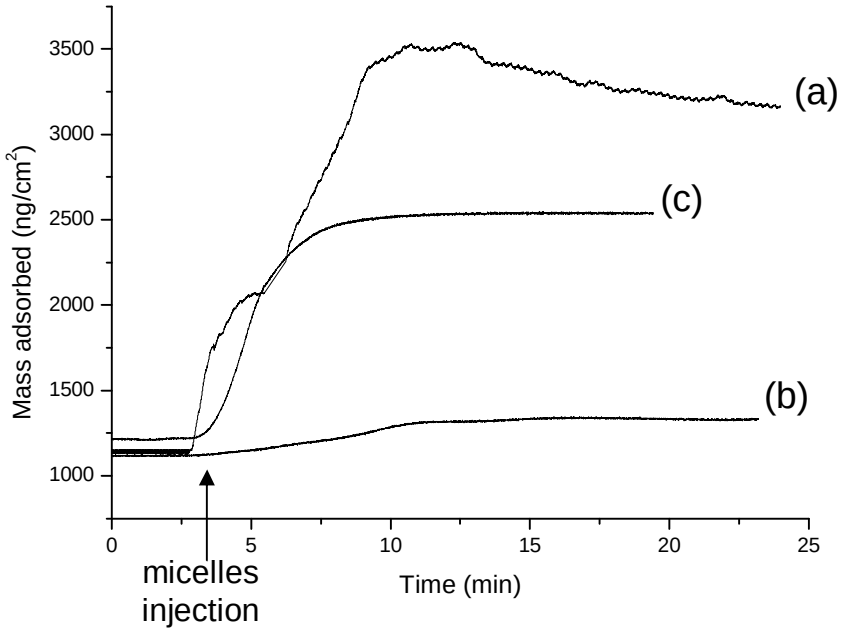
Mass adsorbed (ng/cm^2)
3500
3000
2500
2000
1500
1000
0
5
10
15
20
25
Time (min)
(a)
(c)
(b)
micelles
injection

Figure 9

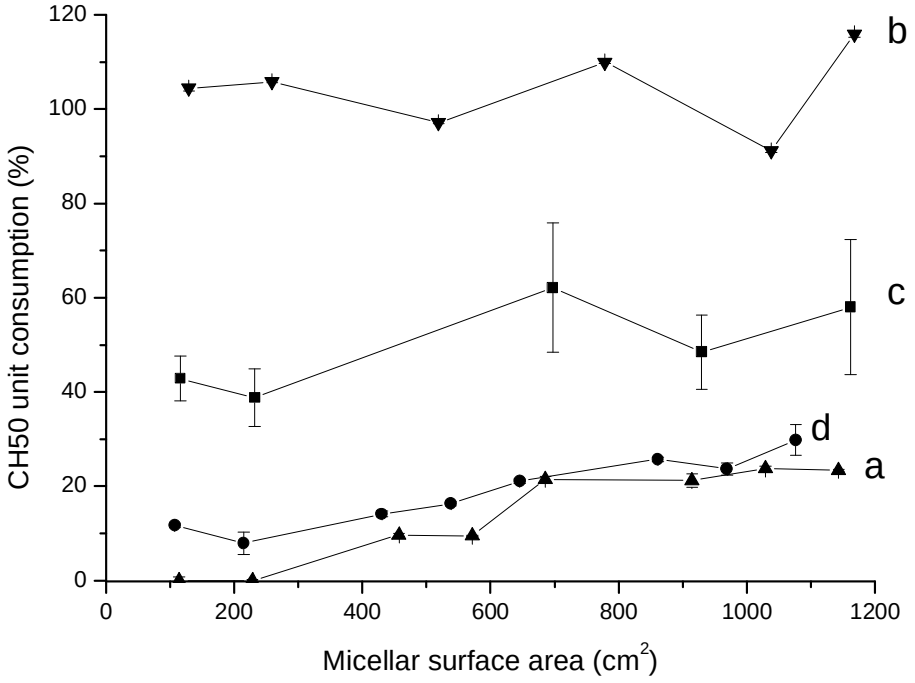
CH50 unit consumption (%)
Micellar surface area (cm2)
0
20
40
60
80
100
120
0
200
400
600
800
1000
1200
b
c
d
a